Geophysical Research Letters

RESEARCH LETTER
10.1029/2019GL084237

Special Section:
The Arctic: An AGU Joint Special Collection

Discharge of Meteoric Water in the Eastern Norwegian Sea since the Last Glacial Period

Wei-Li Hong[1,2], Aivo Lepland[1,2,3], Tobias Himmler[1], Ji-Hoon Kim[4], Shyam Chand[1,2], Diana Sahy[5], Evan A. Solomon[6], James W. B. Rae[7], Tõnu Martma[3], Seung-Il Nam[8], and Jochen Knies[1,2]

[1]Geological Survey of Norway (NGU), Trondheim, Norway, [2]Centre for Arctic Gas Hydrate, Environment and Climate, Arctic University of Norway (UiT), Tromsø, Norway, [3]Department of Geology, Tallinn University of Technology, Tallinn, Estonia, [4]Petroleum & Marine Division, Korea Institute of Geoscience and Mineral Resources, Daejeon, South Korea, [5]British Geological Survey, Nottingham, UK, [6]School of Oceanography, University of Washington, Seattle, WA, USA, [7]School of Earth and Environmental Sciences, University of St. Andrews, St Andrews, UK, [8]Division of Polar Paleoenvironment, Korea Polar Research Institute, Incheon, South Korea

Abstract Submarine groundwater discharge could impact the transport of critical solutes to the ocean. However, its driver(s), significance over geological time scales, and geographical coverage are poorly understood. We characterize a submarine groundwater seep from the continental slope off northern Norway where substantial amount of meteoric water was detected. We reconstruct the seepage history from textural relationships and U-Th geochronology of authigenic minerals. We demonstrate how glacial-interglacial dynamics have promoted submarine groundwater circulation more than 100 km offshore and result in high fluxes of critical solutes to the ocean. Such cryosphere-hydrosphere coupling is likely common in the circum-Arctic implying that future decay of glaciers and permafrost in a warming Arctic is expected to attenuate such a coupled process and thus decreases the export of critical solutes.

Plain Language Summary Occurrence of meteoric groundwater (freshwater originated from precipitation such as rain and snow) in the global ocean is an unexpected but seemingly common phenomenon. Here, we report evidence for meteoric groundwater flow at ~800-m water depth from the coast of northern Norway. Dating of the chemically formed carbonate rocks on the seafloor, an oxidation product of methane, reveals that the groundwater flow was strongest when large ice sheets occupied the nearby shelf. Our results confirm the temporal and geographical scales of meteoric groundwater flow in the Arctic region and highlight its impact on carbon cycling and ocean chemistry.

Key Points:
- We document the connection between glacial dynamics and the discharge of meteoric water from the eastern Norwegian Sea
- A large quantity of critical solutes discharge to the ocean as a result of water circulation
- Offshore presence/discharge of freshwater is a common phenomenon in the circum-Arctic Ocean that have profound impact on ocean chemistry

Supporting Information:
- Supporting Information S1

Correspondence to:
W.-L. Hong,
wei-li.hong@ngu.no

Citation:
Hong, W.-L., Lepland, A., Himmler, T., Kim, J.-H., Chand, S., Sahy, D., et al. (2019). Discharge of meteoric water in the eastern Norwegian Sea Since the last glacial period. *Geophysical Research Letters*, *46*, 8194–8204. https://doi.org/10.1029/2019GL084237

Received 22 JUN 2019
Accepted 25 JUN 2019
Accepted article online 3 JUL 2019
Published online 19 JUL 2019

1. Introduction

Submarine groundwater discharge (SGD) is defined as the discharge of subground fluids across the land-ocean interface that includes a freshwater component (fSGD hereafter) and a recirculated saline groundwater (sSGD hereafter; Taniguchi et al., 2002). Offshore occurrence of freshwater, which may or may not discharge across the land-ocean interface, has also been highlighted recently (e.g., Post et al., 2013). Global estimates suggest that SGD could have a substantial impact on ocean chemistry by conveying trace elements (Charette et al., 2016; Church, 1996; Moore, 1996) and nutrients (Rodellas et al., 2015) from continental shelf sediments to the open oceans. Despite the low water flux of fSGD compared to global river runoff (a few percent at most; Zektser & Loaiciga, 1993; Berner & Berner, 2012; Zhou et al., 2019), its impact on the global geochemical cycle is evident. In addition, SGD in the Arctic has been proposed as one of the processes that transports methane to fjords (Lecher, 2017) and continental shelf environments (Frederick & Buffett, 2016; Lecher et al., 2016), where methane can escape to the atmosphere and result in considerable greenhouse effect. Despite the significance of SGD, our knowledge of its control mechanisms is limited. In the circum-Arctic off Norway, Canada, and Alaska, as well as the Laptev Sea and the Greenland shelf (Figure 1a) where numerous glaciations with episodes of massive ice sheets grounded on the continental shelves occurred over the last 2.7 million years, the dynamics of glaciers and permafrost have been speculated to influence the groundwater flow (DeFoor et al., 2011; Person et al., 2003; Siegel et al., 2014). However, despite these model-based assessments, cryosphere-regulated SGD in the geological past has not been confirmed nor are the temporal/spatial scales of such a process in the Arctic region

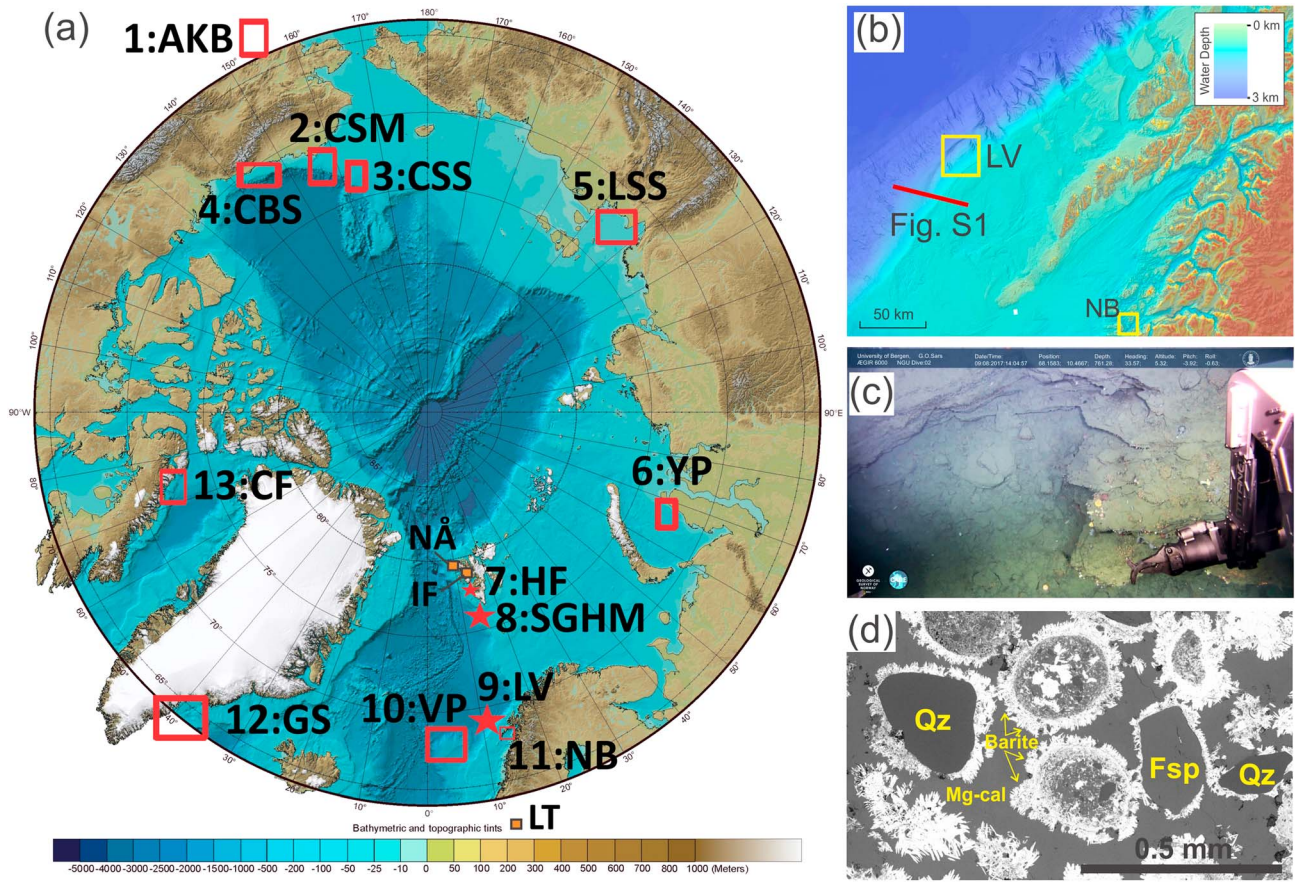

Figure 1. (a) Bathymetry of the circum-Arctic Ocean and locations of reported offshore freshwater and/or fSGD. Stars mark the locations investigated in this study. The three orange squares mark the locations where local meteoric water data are shown in Figure 2 (NÅ: Ny Ålesund; IF: Isfjorden; LT: Lista). 1 = AKB: Alaska Kasitsna Bay (Lecher et al., 2016); 2 = CSM: Canning seafloor mound (Hart et al., 2011; Pohlman et al., 2011); 3 = CSS: Chukchi Sea shelf (Korea Institute of Geoscience and Mineral Resources, 2016); 4 = CBS: Canadian Beaufort Sea (Lecher et al., 2016; Paull et al., 2015); 5 = LSS: Laptev Sea shelf (Charkin et al., 2017); 6 = YP: Yamal Peninsula (Semenov et al., 2019); 7 = HF: Hornsund fjord (this study). 8 = SGHM: Storfjordrenna gas hydrate mounds (this study); 9 = LV: Lofoten-Vesterålen seep (this study); 10 = VP: Vøring Plateau (Aagaard et al., 1989); 11 = NB: Nordbreigrunnen (Storrø, 2012); 12 = GS: Greenland shelf (DeFoor et al., 2011); 13 = CF: Cambridge fjord (Hay, 1984). (b) Detailed bathymetry of the Lofoten-Vesterålen continental margin. The red line marks the seismic profile shown in Figure S1. The yellow squares mark our study region, LV seep, and another freshwater seep, Nordbreigrunnen (NB), ~7 km offshore (Storrø, 2012). Detailed coring locations from the LV seep are shown in Figure S2. (c) A seafloor image from the LV seep with outcrops of horizontal-bedded Eocene sandstones. (d) A scanning electron microscope backscatter image showing that authigenic barite grew first around the detrital quartz (Qz) and feldspar (Fsp) grains with the pore space filled by texturally younger Mg calcite.

clear (Post et al., 2013). Such a gap in knowledge requires immediate attention given the expected warming of the Arctic Ocean (Overland et al., 2014) and associated feedbacks from permafrost decay and glacier retreat on the water cycle.

We report data from a seep at ~800 m below sea level (bsl) on the Lofoten-Vesterålen (LV) continental slope off northern Norway (Figure 1b), where fSGD occurs and meteoric water is transported to the near seafloor sediments. The timing and duration of fSGD are determined through the U-Th dating of authigenic carbonates. Such age information provides a critical constraint on factors controlling the strength of fSGD in the LV seep. We integrate our findings from the LV seep with additional pore fluid data around Svalbard and the circum-Arctic (Figure 1a). We estimate the fluxes of groundwater, methane, and critical solutes from the LV seep through their corresponding pore fluid profiles. Our findings provide a new constraint in the understanding of how cryosphere impact the subsurface groundwater flow and thus the associated solute fluxes to the oceans.

2. Site Descriptions

The LV continental margin offshore northern Norway is a rift margin consisting of three segments (Lofoten, Vesterålen, and Andøya) separated by two transfer zones (Jennengga and Vesterålen; Tsikalas et al., 2001). The result of such rifting is a series of basins and ridges along the LV continental margin (Blystad et al., 1995). Extensive glacial erosion has resulted in very thin to no Quaternary sediment cover over the ridges, where Tertiary and Cretaceous formations are exposed (Tasrianto & Escalona, 2015; Henstra et al., 2017; Figure S1 in the supporting information). Along the continental margin, there are 15 canyons located ~80 km northwest from the Lofoten archipelago with a few of them incised deeply into the Cenozoic sedimentary succession (Rise et al., 2013). Termination of a mafic body formed during the Eocene continental breakup (Breivik et al., 2017) was observed beneath these canyons (Figure S1). Seafloor exploration of two relatively small canyons (not included in Rise et al., 2013; Figures 1b and S2 from the supporting information) with a remotely operated vehicle (ROV) reveal variably lithified, horizontal-bedded sandstone of likely Eocene age (K. Dybkjær, Apr 2019, personal communication) outcropping along the canyon walls at ~800 m bsl (Figure 1c and Table S1 from the supporting information). Abundant microbial mats and seafloor crusts cemented by authigenic sulfates and carbonates (Figure 1d) occur in areas where poorly lithified and coarse-grained strata are exposed (Figure 1c; Sen et al., 2019). Push cores up to 40 cm in length (Table S1 and Figure S2) were recovered by the ROV from microbial mats fringed with siboglinid worms and an area without seafloor bacterial mats (P171-021; Figure S2).

In addition to the LV seep, we document the presence of meteoric water from two locations offshore Svalbard: (1) The Storfjordrenna gas hydrate mounds (SGHMs in Figure 1a) are circular seafloor mounds with a radius of a few hundred meters rising ~10 m above the seafloor south of Svalbard (~380 m bsl). These mounds were investigated for their shallow gas hydrate deposits and intensive methane leakage to the bottom water (Hong et al., 2017; Hong et al., 2018). (2) The Hornsund fjord (HF in Figure 1a) is a 25-km-long and 10-km-wide fjord at the southwestern tip of Spitsbergen. Water depth ranges between roughly 140 to 220 m bsl with the entrance of the fjord being the shallowest. Release of methane from the sediments into the water column has been previously documented with the Hornsund fracture zone as the proposed fluid migration pathway (Damm et al., 2005).

3. Materials and Methods

The sediment cores and seafloor carbonate crusts from the LV seep were collected by ROV Ægir 6000 during the NGU 1710 cruise onboard R/V G.O. Sars in 2017 (Figure S2). The sediment core, CAGE15-2-911GC (Table S1), was recovered from one of the most active Storfjordrenna GHMs (Panieri et al., 2015). The sediment cores HH16-1217GC and HH16-1219GC were collected from the Hornsund fjord during a joint cruise between Korea (Korea Polar Research Institute) and Norway (the Arctic University of Norway, UiT) with R/V Helmer Hanssen in 2016. Details of the recovered HH16-1217GC and HH16-1219GC cores were documented by Forwick et al. (2017). All the methods for the sampling/analyses of pore fluid, solid phases (total organic carbon and seafloor crusts) and headspace gases are given in the supporting information.

4. Results and Discussions

4.1. The Presence and Impact of fSGD from the LV Seep

Pore fluid recovered from the LV seep is characterized by low $\delta^{18}O$ and δD values (as low as −1.7‰ and −7.9‰, respectively) that are 1.9‰ and 10.8‰ lower than the values from bottom seawater (Figures 2a and S4 for the depth profiles). For most of the LV cores, we detected up to 15% lower chloride concentration compared to the bottom seawater (Figure 2b) with a few samples from P1710-052 having chloride content as low as 235 mM (Figure 3). Dehydration of clay minerals is known to release ^{18}O-enriched and ^{2}H-depleted freshwater from the interlayer sites of the minerals (Kastner et al., 1991; Sheppard & Gilg, 1996; Dählmann & De Lange, 2003; Hensen et al., 2004; Table S2 from the supporting information). Gas hydrate concentrates heavy isotopes (^{18}O and ^{2}H) in the lattice (Maekawa, 2004); dissociation of hydrate therefore releases freshwater enriched in both ^{18}O and ^{2}H (Tomaru et al., 2006; Table S2). Neither process can explain the ^{18}O- and ^{2}H-depleted pore fluid that is fresher than seawater from the LV sites. Both anaerobic oxidation of methane (AOM) and microbial methanogenesis fractionate only hydrogen isotopes when oxidizing methane to water (or reducing methane for microbial

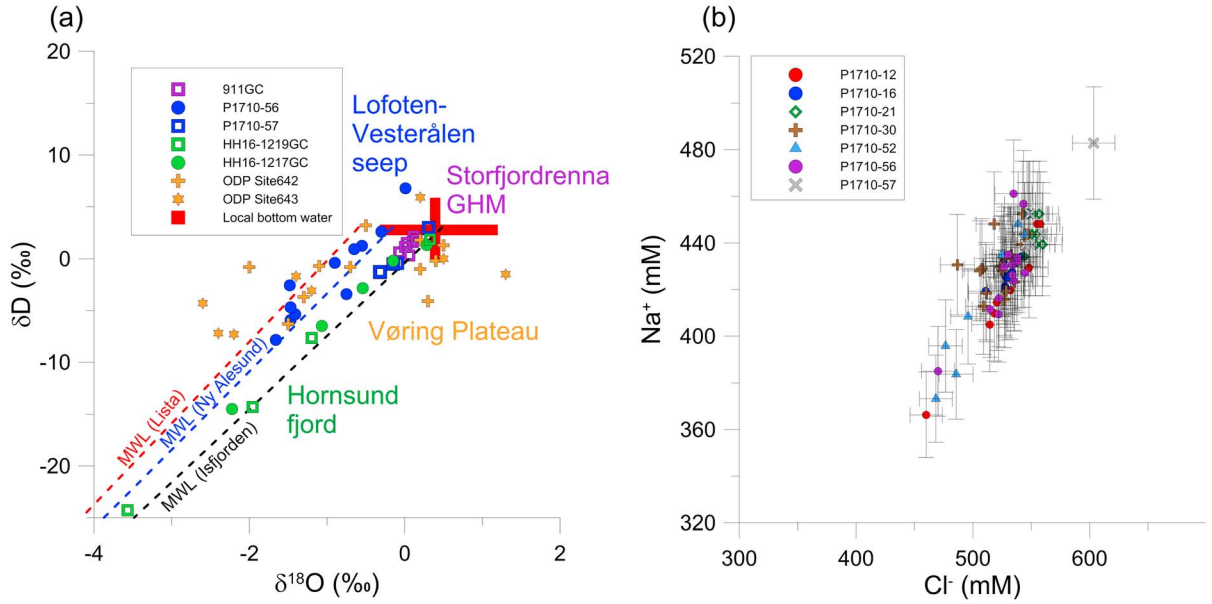

Figure 2. The presence of meteoric water as inferred from the stable isotopes of the pore fluid as well as the concentrations of dissolved chloride (Cl^-) and sodium (Na^+). (a) Stable oxygen and hydrogen isotopic ratios of pore fluid from the four locations: LV seep, Storfjordrenna gas hydrate mounds (GHMs), Hornsund fjord and Vøring plateau (Aagaard et al., 1989; see Figure 1a for locations). These data overlap with three local meteoric water lines from mainland Norway (Lista) and Svalbard (Isfjorden and Ny Ålesund; see Figure 1a for locations). The meteoric water lines were derived based on the regressions from the isotopic composition of precipitation since 1960 (International Atomic Energy Agency, 2018). The raw data used for regression and the comparison with our pore fluid isotopic compositions are shown in Figure S3 from the supporting information. The red cross marks the ranges of isotopic values for different water masses (Voelker et al., 2015) with the center depicts the values for local bottom water. (b) A cross plot of dissolved sodium and chloride concentrations of seven cores from the LV seep. We detected chloride and sodium concentrations as low as 235 and 330 mM, respectively, from core P1710-52 (Figure 3). These anomalous data are however not included in (b) as they were not measured from the same sample due to the low yield of porewater from this core.

methanogenesis; Valentine et al., 2004; Holler et al., 2009; Table S2). Spatial and temporal variations in seawater isotopic composition can also be ruled out due to the much smaller differences among water masses (1.5‰ for $\delta^{18}O$ and 6‰ for δD from Figure 2a; Voelker et al., 2015) and the higher $\delta^{18}O$ isotopic values of seawater by 0.4‰ to 0.6‰ during the Last Glacial Maximum (Adkins et al., 2002). The correspondence between our pore fluid data and the three meteoric water lines (Figure 2a) suggests a significant contribution of meteoric water to the pore fluid.

From the dissolved boron profiles, we estimated linear velocities of water migration to be between 0.1 and 0.25 m/year (Figure 3) with water fluxes ranging between 0.063 and 0.195 m^3/m^2/year (see the supporting information for details). The estimated water fluxes are similar to those from the locations with comparable water depths such as North Slope Alaska, NE coastal Gulf of Mexico, and Sagami Bay Japan (Taniguchi et al., 2002, and references therein). Despite the significant fSGD revealed by our results, the pore fluid comprises primarily seawater. The high chloride content in the pore fluid (Figures 2b and 3) can be explained by the significant seawater contribution (i.e., sSGD) due to the seawater-freshwater exchange in aquifers (Taniguchi et al., 2002). The fluid exchange across sediment-water interface as a result of tidal pressure was also proposed to explain the large sSGD contribution (Moore & Wilson, 2005), which is, however, not applicable to LV seep due to the great water depth.

Abundant boron, lithium, and barium were transported by groundwater resulting in the high concentrations detected in the pore fluid from the LV seep (Figure 3 and Figure S4 from the supporting information). Notably, the pore fluid contains up to 1 mM of barium (Figure 3), 1 to 3 orders of magnitude higher than the values previously reported (Nähr & Bohrmann, 1999; Solomon & Kastner, 2012; Torres et al., 2002). Primary barium sources include rivers (Guay & Falkner, 1998), hydrothermal venting (Von Damm et al., 1985), sedimentary barite dissolution (Solomon & Kastner, 2012), and alteration of mafic igneous rocks (Humphris & Thompson, 1978). Given the local geology of the LV area and the occurrence of a mafic body (Figure S1), barium leaching from igneous rocks is the most likely explanation for such high concentrations.

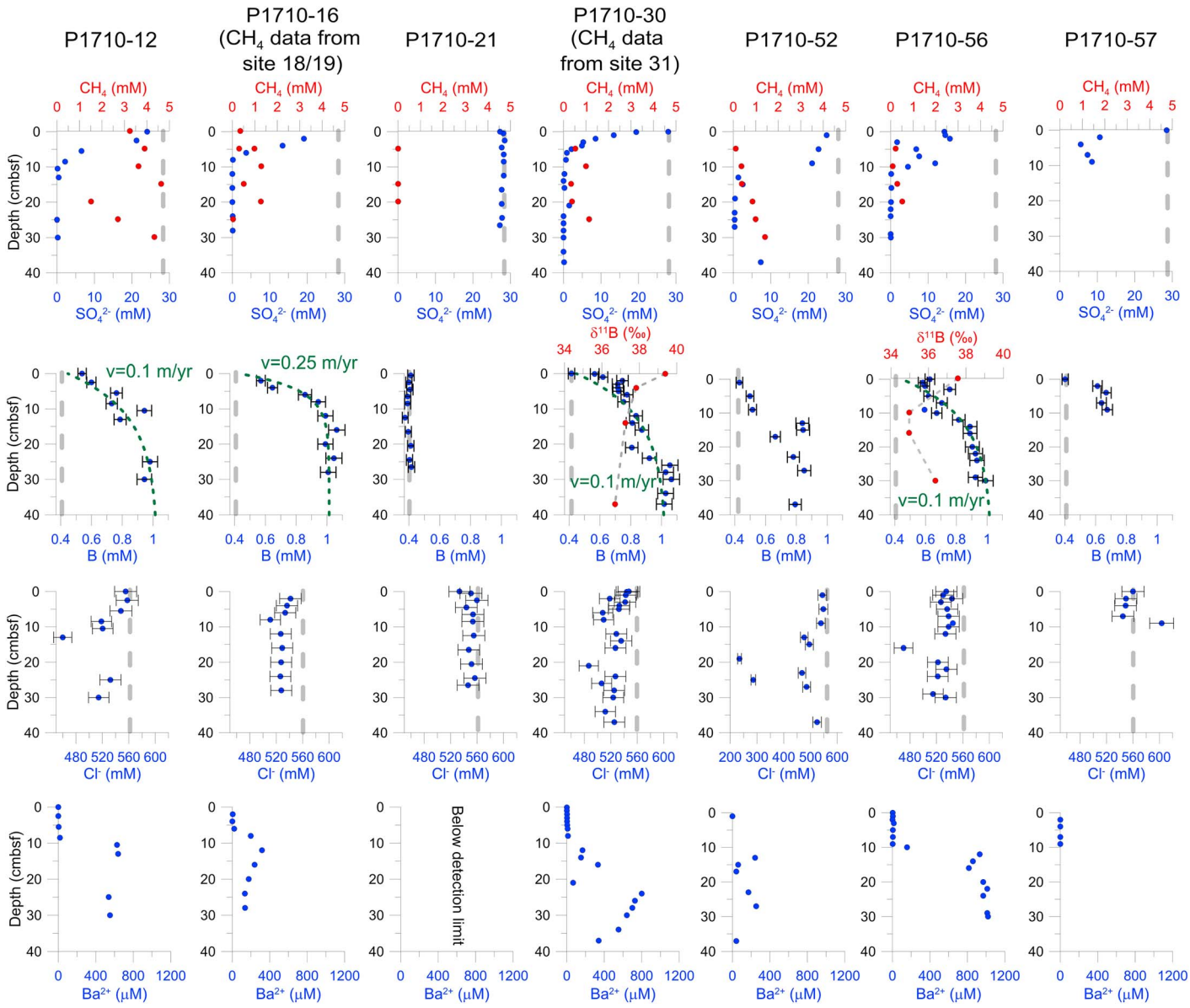

Figure 3. Pore fluid methane, sulfate, boron, and chloride concentration profiles with two selected sites with $\delta^{11}B$ signatures. Gray dash lines mark the seawater concentrations of sulfate, boron, and chloride. Note the different scale of chloride concentration for P1710-52. The analytical uncertainties for sulfate and barium concentrations as well as $\delta^{11}B$ are smaller than the symbols.

The abundant dissolved calcium and silica as well as the low magnesium and potassium concentrations in the pore fluid (Figures S4 and S5 from the supporting information) are consistent with the interaction between pore fluid and mafic rocks (Aagaard et al., 1989). The lithium-based geochemical thermometer (Kharaka & Mariner, 1989) suggests equilibrium temperature between 19 and 32 °C (Table S3). When assigning the subsurface temperature derived from a 3-D thermal model in the region (Maystrenko, Gernigon, 2018), this range of temperature corresponds well to the depth of the observed mafic body (~1 km, Figure S1). We acknowledge the large uncertainties of the geochemical thermometers which may underestimate the temperature by 80% in extreme cases (Ferguson et al., 2009). However, our estimated equilibrium temperature of fluid is supported by the 3–5‰ lighter $\delta^{11}B$ signal measured (Figure 3), indicating desorption of boron from clay minerals with elevated subsurface temperature. For example, You et al. (1996) demonstrated that an initial 38 °C heating of pelagic marine sediments could result in up to 10‰ decrease in the $\delta^{11}B$ value of the solution.

High concentrations of methane were detected at the sediment-water interface in a few cores (Figure 3) that we propose were produced locally through microbial methanogenesis in the shallow subsurface. The high ammonium concentration (up to 1.13 mM), ^{13}C-depleted isotopic signature of methane (−80.3‰ to −115.9% Vienna Pee Dee belemnite), and the downcore decrease in total organic carbon content (Figures S5 to S7 from the supporting information) suggest in situ microbial organoclastic methanogenesis in the cored depths. The produced methane stimulates AOM (Boetius et al., 2000), which is responsible for the rapid decline in sulfate concentration (Figure 3). The alkalinity production through AOM (Figure S5) promotes authigenic carbonate (Mg-calcite and aragonite) precipitation (Figure 1d) as suggested by their low δ^{13}C (−49.6‰ to −64.3‰ Vienna Pee Dee belemnite; Table S4 from the supporting information).

4.2. The Mechanism Regulating fSGD at the LV Seep

The fSGD at the LV seep may be explained by (1) modern circulation of groundwater from the Lofoten archipelago or even mainland Norway as proposed by Maystrenko, Broenner, et al. (2018) for the freshwater seep from Nordbreigrunnen (NB in Figure 1) or (2) past groundwater circulation as a consequence of glacial-interglacial dynamics (e.g., DeFoor et al., 2011; Person et al., 2003; Siegel et al., 2014). Here, we argue for the latter since our investigations of the seafloor authigenic carbonate crusts suggest that the seepage at the LV seep has been active, and likely stronger, in the geological past. Through microscopic inspection, we observed authigenic barite precipitated around the detrital mineral grains with carbonates formed in the pore space among these barite-coated grains (Figure 1d). Such textural relationship suggests that precipitation of barite preceded the formation of the ^{13}C-depleted carbonates. Precipitation of authigenic barite occurs at the sediment depth where pore fluid sulfate is nearly exhausted and dissolved barium concentration starts to increase (Torres et al., 1996). The appearance of abundant authigenic barite in the seafloor crusts (Figure 1d) suggests such interface was closer to the sediment-water interface in the past than the modern depth between 6 and 15 cm bsf as inferred from the pore fluid profiles (Figure 3). The shallower depth of authigenic barite formation indicates higher dissolved barium flux as a result of greater fSGD in the past. The U-Th ages of the texturally later carbonates provide constraints for the timing of fSGD. The ages are mostly younger than ~22 ka BP (kilo years before 1950) with a few significant older ages from ~50 to 81 ka BP (Figure 4a and Table S5 from the supporting information). In addition, 12 out of 15 of the ages correspond to periods when the volume of the NE Eurasian ice sheets was decreasing or relatively small (i.e., deglaciation and interglacial periods; Figure 4a). These dating results confirm that fSGD has been active at least over the last 22 ka. Though it is difficult to completely exclude, modern groundwater infiltration (e.g., Befus et al., 2017; Jasechko et al., 2017) as the sole cause for the observed water isotopic signal is unlikely.

We propose that, during the Last Glacial Maximum, the great pressure contrast between land and ocean as a result of the 900-m-thick glacier (Patton et al., 2016) and 120 m lower sea level (Waelbroeck et al., 2002) created the hydraulic pressure for the meltwater at the base of glaciers to infiltrate into the exposed permeable strata and flowed toward the ocean (Figure 4b). This could likely occur at the top of the basement high where erosion by ice sheet was the most intensive, for example, Røst High that is ~30 km east of the LV seeps (Figures 4b and 4c). The results of shallow drilling and seismic data from the LV margin indicate the occurrence of interbedded strata of Tertiary sandstone/conglomerate and mudstone with variable permeability (Hansen et al., 1992; Henstra et al., 2017; Tasrianto & Escalona, 2015; Tsikalas et al., 2001), which are the most likely conduits for the observed fSGD. The fine-grained interbed in this Tertiary bed potentially serves as the confined layer that maintains the overpressure condition and guides the groundwater flow. Indeed, the findings of interbedded Eocene sandstone/mudstone exposed on the flanks of the LV canyons (Figure 1c) with methane seepage related microbial colonies associating with coarse-grained strata (Sen et al., 2019) support this conclusion. The fracture zone observed beneath the LV seep from the seismic profile (Figure S1) also provides the pathway for fluid to migrate from the Paleocene-Miocene strata. Similar cryosphere-controlled SGD were documented from the Greenland shelf (DeFoor et al., 2011) and Atlantic continental shelf offshore the northeastern United States (Person et al., 2003) with freshwater flow two orders of magnitude faster than what we estimated from the LV seep at present day. Under the conditions of decaying glaciers and rising sea level, the strength of such water circulation decreased as the gradient of hydraulic head could not be maintained (Figure 4c). It has been shown that the retreat of the subsurface freshwater front was not homogenous but occurred over several thousand years for a distance of 100 km, with pockets of freshwater still present far offshore 15 ka after the deglaciation (Siegel et al., 2014).

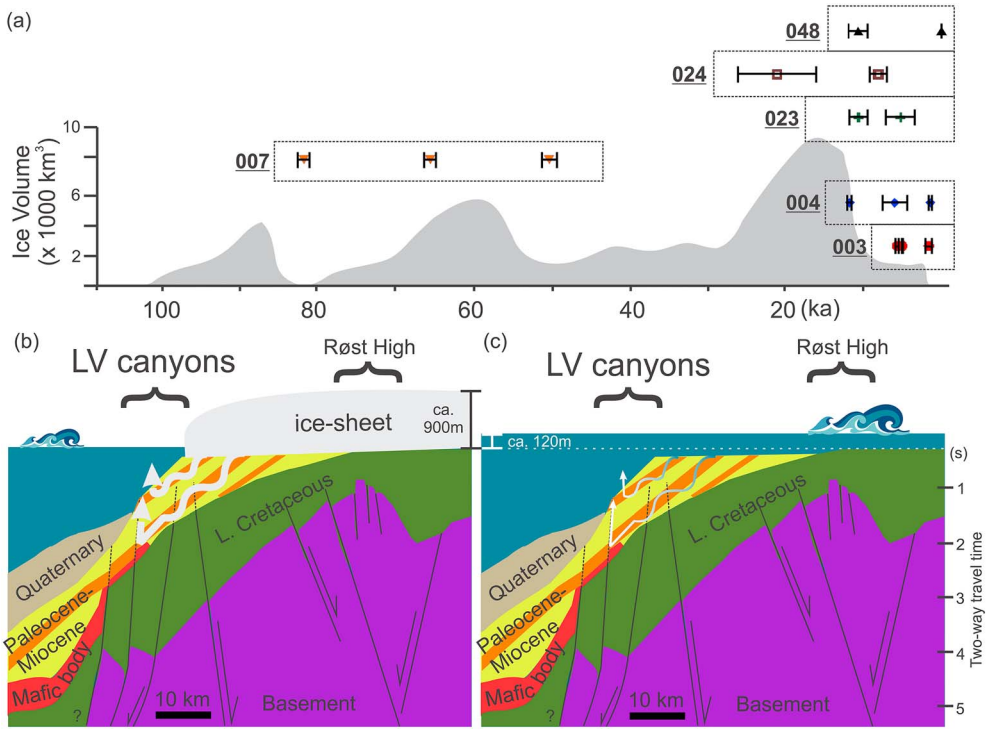

Figure 4. Timing and the proposed flow path for the freshwater component submarine groundwater discharge (fSGD) as a result of glacial-interglacial dynamics at the Lofoten-Vesterålen (LV) seep. (a) Variation of NE Eurasian ice sheet volume from Svendsen et al. (2004) (gray shaded area corresponding to the left *y* axis) was compared with our U-Th ages derived from authigenic carbonates (note the wide range of dates from sample 007 which is unusual). Most of the ages correspond to deglaciation and interglacial periods. (b, c) Proposed flow path for fSGD during glaciation and present. Subsurface geology was adapted from Tasrianto and Escalona (2015) with modifications according to Tsikalas et al. (2001), Henstra et al. (2017), and the seismic profile Figure S1. We propose that the Tertiary sandstone layers (orange beds in the Paleocene-Miocene strata), that are exposed on the seafloor in the canyon (Figure 1c), serve as the conduit for fSGD with the fine-grained interbeds (yellow beds in Paleocene-Miocene strata) serve as the confined layers. The thick ice sheet and lower sea level (e.g., in panel b) provide the hydraulic motivation for a greater fSGD. In the present day, higher sea level and the disappearance of the ice sheet results in a smaller fSGD with substantial seawater contribution as indicated by the high chloride content in the pore fluid (Figure 2b).

4.3. Implications of the circum-Arctic Ocean fSGD

From the observations of pore fluid and authigenic minerals at the LV seep, we argue that the fSGD with significant contribution from meteoric water could occur over geological time scales and extend to the modern continental slope. This interpretation is consistent with the modeling work, which also highlights the importance of specific geological conditions as the reason for the presence of SGD so far offshore (Michael et al., 2016). Occurrence of meteoric freshwater is likely common in the formerly glaciated Norwegian continental margin as suggested by the low $\delta^{18}O$ and δD values of pore fluid from Storfjordrenna GHM and Hornsund fjord, as well as from Vøring Plateau (Ocean Drilling Program Sites 642 and 643; Aagaard et al., 1989; Figures 2a and Figure S3). By compiling existing observations of fSGD and offshore freshwater occurrence from the literatures (Figure 1a), we conclude that such observations are common in the circum-Arctic Ocean. Jasechko (2016) showed that the lower $\delta^{18}O$ value in Pleistocene groundwater compared to Holocene groundwater from higher latitude toward the North Pole reflects both the greater Rayleigh distillation effect in the cooler Pleistocene polar air masses and the greater contribution from the glacier-sourced groundwater around the major ice sheet in the Northern Hemisphere. Future work is needed to examine whether similar glacial-interglacial perturbation can explain the occurrence of freshwater and/or fSGD in the circum-Arctic Ocean, as we demonstrated for the LV seep.

The feedback between cryosphere and hydrosphere not only controls the seawater-freshwater interface but also influences carbon cycling and ocean chemistry. The estimated methane flux from the LV seep based on the measured methane concentration and present water velocity ranges from 3.5 to 30.0 μmole/cm^2/year

(Table S6 from the supporting information). These fluxes are comparable to the methane flux calculated from Prins Karls Forland, west of Svalbard, as a result of gas hydrate dissociation 6–8 ka ago (Wallmann et al., 2018). If we assume the pore fluid is saturated with methane, the flux can be as high as 875 μmole/cm^2/year (Table S6) or comparable to the estimation from methane gas bubbling in the water column from Prins Karls Forland (Sahling et al., 2014). The high methane concentrations detected at the sediment-water interface (Figure 3) suggest the saturated capacity of AOM and active methane escape to the bottom water enhanced by fSGD. Such a methane transport process has been largely overlooked (James et al., 2016) and warrants future research to assess its regional significance. The present advective flux of barium toward the depth of sulfate-methane transition at the LV seep is 2.4–7.1 μmole/cm^2/year (Table S6) or comparable to the benthic fluxes measured elsewhere (McManus et al., 1998). For elements such as boron and lithium, the present advective fluxes to the bottom water are as high as 17.6 and 0.7 μmole/cm^2/year, respectively (Table S6). At places where thick ice sheets are still present, such as Greenland and Antarctica (Uemura et al., 2011), future glacier retreat is expected to impact the fluxes of methane and other solutes due to the similar hydrological driver as observed along the eastern Norwegian Sea.

5. Conclusions

We have documented fSGD from the LV continental slope with discharges of meteoric water and critical solutes. The U-Th ages of authigenic seep carbonates indicate that fSGD has been active since at least 22,000 years ago. We propose that the strength of fSGD is controlled by the hydraulic head contrast reflecting the advance/retreat of glaciers onto the continental shelf and sea level fluctuations during the glacial-interglacial periods. By integrating the LV results with additional pore fluid data around the Svalbard archipelago and the circum-Arctic Ocean, we propose that the presence of offshore freshwater and/or fSGD is a common phenomenon in the Arctic Ocean and contributes significant amounts of critical solutes to the ocean.

Acknowledgments
We acknowledge the captain, crew members, and ROV operators during the NGU cruise 1710 onboard R/V G.O. SARS for assistance. We appreciate the help from Ms. Haoyi Yao for shipboard sampling, lab technicians from NGU for analyses, and Ms. Aave Lepland for helping with maps. The work is supported by the Research Council of Norway (RCN) through Petromaks2-NORCRUST (project 255150) and its Centre of Excellence funding scheme for CAGE (project 223259). J.-H. K. is supported by the project "Development on Geochemical Proxies of Isotope and Trace Element for Understanding of Earth and Universe Evolution Processes (GP2017-018)" funded by the Korea Ministry of Science and ICT (MSIT). Svalbard fjord cruise in 2016 with RV Helmer Hanssen for Science Research Program to S.-I. N. is fully supported by MSIT (NRF-2015M1A5A1037243, PN19090). We also acknowledge the three anonymous reviewers for their thorough and insightful reviews. All data reported in this manuscript can be found from the supporting information.

References

Aagaard, P., P. K. Egeberg and P. C. Smalley (1989). Diagenetic reactions in Leg 104 sediments inferred from isotope and major element chemistry of interstitial waters. Proc. ODP, Sci. Results, Citeseer. https://doi.org/10.2973/odp.proc.sr.104.122.1989

Adkins, J. F., McIntyre, K., & Schrag, D. P. (2002). The salinity, temperature, and δ18O of the glacial deep ocean. *Science*, *298*(5599), 1769–1773. https://doi.org/10.1126/science.1076252

Befus, K. M., Jasechko, S., Luijendijk, E., Gleeson, T., & Bayani Cardenas, M. (2017). The rapid yet uneven turnover of Earth's groundwater. *Geophysical Research Letters*, *44*, 5511–5520. https://doi.org/10.1002/2017GL073322

Berner, E. K., & Berner, R. A. (2012). *Global environment: water, air, and geochemical cycles*. Princeton University Press.

Blystad, P., Brekke, H., Færseth, R. B., Largsen, B. T., Skogseid, J., & Tørudbakken, B. (1995). Structural elements of the Norwegian continental shelf. Part 2: The Norwegian Sea region. *NPD Bull*, *8*.

Boetius, A., Ravenschlag, K., Schubert, C. J., Rickert, D., Widdel, F., Gieseke, A., et al. (2000). A marine microbial consortium apparently mediating anaerobic oxidation of methane. *Nature*, *407*(6804), 623–626. https://doi.org/10.1038/35036572

Breivik, A. J., Faleide, J. I., Mjelde, R., Flueh, E. R., & Murai, Y. (2017). A new tectono-magmatic model for the Lofoten/Vesterålen Margin at the outer limit of the Iceland Plume influence. *Tectonophysics*, *718*, 25–44. https://doi.org/10.1016/j.tecto.2017.07.002

Charette, M. A., Lam, P. J., Lohan, M. C., Kwon, E. Y., Hatje, V., Jeandel, C., et al. (2016). Coastal ocean and shelf-sea biogeochemical cycling of trace elements and isotopes: lessons learned from GEOTRACES. *Philosophical Transactions of the Royal Society A: Mathematical, Physical and Engineering Sciences*, *374*(2081). https://doi.org/10.1098/rsta.2016.0076

Charkin, A. N., Van Der Loeff, M. R., Shakhova, N. E., Gustafsson, Ö., Dudarev, O. V., Cherepnev, M. S., et al. (2017). Discovery and characterization of submarine groundwater discharge in the Siberian Arctic seas: a case study in the Buor-Khaya Gulf, Laptev Sea. *The Cryosphere*, *11*(5), 2305–2327. https://doi.org/10.5194/tc-11-2305-2017

Church, T. M. (1996). An underground route for the water cycle. *Nature*, *380*(6575), 579–580. https://doi.org/10.1038/380579a0

Dählmann, A., & De Lange, G. (2003). Fluid–sediment interactions at Eastern Mediterranean mud volcanoes: a stable isotope study from ODP Leg 160. *Earth And Planetary Science Letters*, *212*(3-4), 377–391. https://doi.org/10.1016/S0012-821X(03)00227-9

Damm, E., Mackensen, A., Budéus, G., Faber, E., & Hanfland, C. (2005). Pathways of methane in seawater: Plume spreading in an Arctic shelf environment (SW-Spitsbergen). *Continental Shelf Research*, *25*(12-13), 1453–1472. https://doi.org/10.1016/j.csr.2005.03.003

DeFoor, W., Person, M., Larsen, H. C., Lizarralde, D., Cohen, D., & Dugan, B. (2011). Ice sheet–derived submarine groundwater discharge on Greenland's continental shelf. *Water Resources Research*, *47*, W07549. https://doi.org/10.1029/2011WR010536

Ferguson, G., Grasby, S., & Hindle, S. (2009). What do aqueous geothermometers really tell us? *Geofluids*, *9*(1), 39–48. https://doi.org/10.1111/j.1468-8123.2008.00237.x

Forwick, M., S.-I. Nam, K. Husum and S. Iversen (2017). "2016 RV Helmer Hanssen cruise report: Marine-geological cruise to west Spitsbergen fjords."

Frederick, J. M., & Buffett, B. A. (2016). Submarine groundwater discharge as a possible formation mechanism for permafrost-associated gas hydrate on the circum-Arctic continental shelf. *Journal of Geophysical Research: Solid Earth*, *121*, 1383–1404. https://doi.org/10.1002/2015JB012627

Guay, C., & Falkner, K. K. (1998). A survey of dissolved barium in the estuaries of major Arctic rivers and adjacent seas. *Continental Shelf Research*, *18*(8), 859–882. https://doi.org/10.1016/S0278-4343(98)00023-5

Hansen, J., S. Bakke, S. Fanavoll, H. Løseth, A. Mørk, M. Mørk, et al. (1992). "Shallow drilling Nordland VI and VII 1991—main report." IKU report 23: 00-02.

Hart, P. E., J. W. Pohlman, T. D. Lorenson and B. D. Edwards (2011). Beaufort Sea Deep-water gas hydrate recovery from a seafloor mound in a region of widespread BSR occurence. Proceedings of the 7th International Conference on Gas Hydrates (ICGH 2011), Edinburgh, Scotland.

Hay, A. E. (1984). Remote acoustic imaging of the plume from a submarine spring in an Arctic fjord. *Science*, *225*(4667), 1154–1156. https://doi.org/10.1126/science.225.4667.1154

Hensen, C., Wallmann, K., Schmidt, M., Ranero, C. R., & Suess, E. (2004). Fluid expulsion related to mud extrusion off Costa Rica—A window to the subducting slab. *Geology*, *32*(3), 201–204. https://doi.org/10.1130/G20119.1

Henstra, G. A., Gawthorpe, R. L., Helland-Hansen, W., Ravnås, R., & Rotevatn, A. (2017). Depositional systems in multiphase rifts: seismic case study from the Lofoten margin, N orway. *Basin Research*, *29*(4), 447–469. https://doi.org/10.1111/bre.12183

Holler, T., Wegener, G., Knittel, K., Boetius, A., Brunner, B., Kuypers, M. M. M., & Widdel, F. (2009). Substantial C-13/C-12 and D/H fractionation during anaerobic oxidation of methane by marine consortia enriched in vitro. *Environmental Microbiology Reports*, *1*(5), 370–376. https://doi.org/10.1111/j.1758-2229.2009.00074.x

Hong, W.-L., Torres, M. E., Carroll, J., Crémière, A., Panieri, G., Yao, H., & Serov, P. (2017). Seepage from an arctic shallow marine gas hydrate reservoir is insensitive to momentary ocean warming. *Nature communications*, *8*(1), 15745. https://doi.org/10.1038/ncomms15745

Hong, W.-L., Torres, M. E., Portnov, A., Waage, M., Haley, B., & Lepland, A. (2018). Variations in gas and water pulses at an Arctic seep: fluid sources and methane transport. *Geophysical Research Letters*, *45*, 4153–4162. https://doi.org/10.1029/2018GL077309

Humphris, S. E., & Thompson, G. (1978). Trace element mobility during hydrothermal alteration of oceanic basalts. *Geochimica Et Cosmochimica Acta*, *42*(1), 127–136. https://doi.org/10.1016/0016-7037(78)90222-3

International Atomic Energy Agency (2018). "Global Network of Isotopes in Precipitation." The GNIP Database: https://nucleus.iaea.org/wiser.

James, R. H., Bousquet, P., Bussmann, I., Haeckel, M., Kipfer, R., Leifer, I., et al. (2016). Effects of climate change on methane emissions from seafloor sediments in the Arctic Ocean: A review. *Limnology and Oceanography*, *61*(S1), S283–S299. https://doi.org/10.1002/lno.10307

Jasechko, S. (2016). Late-Pleistocene precipitation δ18O interpolated across the global landmass. *Geochemistry, Geophysics, Geosystems*, *17*, 3274–3288. https://doi.org/10.1002/2016GC006400

Jasechko, S., Perrone, D., Befus, K. M., Cardenas, M. B., Ferguson, G., Gleeson, T., et al. (2017). Global aquifers dominated by fossil groundwaters but wells vulnerable to modern contamination. *Nature Geoscience*, *10*(6), 425–429. https://doi.org/10.1038/ngeo2943

Kastner, M., Elderfield, H., & Martin, J. B. (1991). Fluids in convergent margins: What do we know about their composition, origin, role in diagenesis and importance for oceanic chemical fluxes? *Philosophical Transactions: Physical Sciences and Engineering*, *335*(1638), 243–259.

Kharaka, Y. K., & Mariner, R. H. (1989). *Chemical geothermometers and their application to formation waters from sedimentary basins. Thermal history of sedimentary basins* (pp. 99–117). Springer. https://doi.org/10.1007/978-1-4612-3492-0_6

Korea Institute of Geoscience and Mineral Resources (2016). Preliminary survey for marine energy resources in the Arctic region GP2015-041-2016(2). **:** 234.

Lecher, A. (2017). Groundwater discharge in the Arctic: A review of studies and implications for biogeochemistry. *Hydrology*, *4*(3), 41. https://doi.org/10.3390/hydrology4030041

Lecher, A. L., Kessler, J., Sparrow, K., Garcia-Tigreros Kodovska, F., Dimova, N., Murray, J., et al. (2016). Methane transport through submarine groundwater discharge to the North Pacific and Arctic Ocean at two Alaskan sites. *Limnology and Oceanography*, *61*(S1).

Maekawa, T. (2004). Experimental study on isotopic fractionation in water during gas hydrate formation. *Geochemical Journal*, *38*(2), 129–138. https://doi.org/10.2343/geochemj.38.129

Maystrenko, Y. P., M. Broenner, O. Olesen, T. Saloranta and T. Slagstad (2018). Is intraplate seismicity in Norway related to elevated atmospheric precipitation rates and low-velocity upper mantle? AGU Fall Meeting Abstracts.

Maystrenko, Y. P., Gernigon, L., Olesen, O., Ottesen, D., & Rise, L. (2018). 3D thermal effect of late Cenozoic erosion and deposition within the Lofoten-Vesterålen segment of the Mid-Norwegian continental margin. *Geophysical Journal International*, *213*(2), 885–918. https://doi.org/10.1093/gji/ggy013

McManus, J., Berelson, W. M., Klinkhammer, G. P., Johnson, K. S., Coale, K. H., Anderson, R. F., et al. (1998). Geochemistry of barium in marine sediments: Implications for its use as a paleoproxy. *Geochimica Et Cosmochimica Acta*, *62*(21-22), 3453–3473. https://doi.org/10.1016/S0016-7037(98)00248-8

Michael, H. A., Scott, K. C., Koneshloo, M., Yu, X., Khan, M. R., & Li, K. (2016). Geologic influence on groundwater salinity drives large seawater circulation through the continental shelf. *Geophysical Research Letters*, *43*, 10,782–10,791. https://doi.org/10.1002/2016GL070863

Moore, W. S. (1996). Large groundwater inputs to coastal waters revealed by 226Ra enrichments. *Nature*, *380*(6575), 612–614. https://doi.org/10.1038/380612a0

Moore, W. S., & Wilson, A. M. (2005). Advective flow through the upper continental shelf driven by storms, buoyancy, and submarine groundwater discharge. *Earth And Planetary Science Letters*, *235*(3-4), 564–576. https://doi.org/10.1016/j.epsl.2005.04.043

Nähr, T. H., & Bohrmann, G. (1999). Barium-rich authigenic clinoptilolite in sediments from the Japan Sea—A sink for dissolved barium? *Chemical Geology*, *158*(3-4), 227–244. https://doi.org/10.1016/S0009-2541(99)00051-0

Overland, J. E., Wang, M., Walsh, J. E., & Stroeve, J. C. (2014). Future Arctic climate changes: Adaptation and mitigation time scales. *Earth's Future*, *2*(2), 68–74. https://doi.org/10.1002/2013EF000162

Panieri, G., W. G. J. Ambrose, E. K. L. Åström, M. Carroll, D. J. Fornari and e. al. (2015). "Cruise Report CAGE 15-2: Gas hydrate deposits and methane seepages offshore western Svalbard and Storfjordrenna Biogeochemical and biological investigations." from https://cage.uit.no/wp-content/uploads/2019/02/15-2.cage-cruise-report-public-1.pdf.

Patton, H., Hubbard, A., Andreassen, K., Winsborrow, M., & Stroeven, A. P. (2016). The build-up, configuration, and dynamical sensitivity of the Eurasian ice-sheet complex to Late Weichselian climatic and oceanic forcing. *Quaternary Science Reviews*, *153*, 97–121. https://doi.org/10.1016/j.quascirev.2016.10.009

Paull, C. K., Dallimore, S. R., Caress, D. W., Gwiazda, R., Melling, H., Riedel, M., et al. (2015). Active mud volcanoes on the continental slope of the Canadian Beaufort Sea. *Geochemistry, Geophysics, Geosystems*, *16*, 3160–3181. https://doi.org/10.1002/2015GC005928

Person, M., Dugan, B., Swenson, J. B., Urbano, L., Stott, C., Taylor, J., & Willett, M. (2003). Pleistocene hydrogeology of the Atlantic continental shelf, New England. *Geological Society of America Bulletin*, *115*(11), 1324–1343. https://doi.org/10.1130/B25285.1

Pohlman, J., T. Lorenson, P. Hart, C. Ruppel, C. Joseph, M. Torres and B. Edwards (2011). Evidence for freshwater discharge at a gas hydrate-bearing seafloor mound on the Beaufort Sea continental slope. AGU Fall Meeting Abstracts.
Post, V. E., Groen, J., Kooi, H., Person, M., Ge, S., & Edmunds, W. M. (2013). Offshore fresh groundwater reserves as a global phenomenon. *Nature*, *504*(7478), 71–78. https://doi.org/10.1038/nature12858
Rise, L., Bøe, R., Riis, F., Bellec, V. K., Laberg, J. S., Eidvin, T., et al. (2013). The Lofoten-Vesterålen continental margin, North Norway: canyons and mass-movement activity. *Marine and Petroleum Geology*, *45*, 134–149. https://doi.org/10.1016/j.marpetgeo.2013.04.021
Rodellas, V., Garcia-Orellana, J., Masqué, P., Feldman, M., & Weinstein, Y. (2015). Submarine groundwater discharge as a major source of nutrients to the Mediterranean Sea. *Proceedings of the National Academy of Sciences*, *112*(13), 3926–3930. https://doi.org/10.1073/pnas.1419049112
Sahling, H., Römer, M., Pape, T., Bergès, B., dos Santos Fereirra, C., Boelmann, J., et al. (2014). Gas emissions at the continental margin west off Svalbard: mapping, sampling, and quantification. *Biogeosciences Discussions*, *11*(5), 7189–7234. https://doi.org/10.5194/bgd-11-7189-2014
Semenov, P., Portnov, A., Krylov, A., Egorov, A., & Vanshtein, B. (2019). Geochemical evidence for seabed fluid flow linked to the subsea permafrost outer border in the South Kara Sea. *Geochemistry*. https://doi.org/10.1016/j.chemer.2019.04.005
Sen, A., Himmler, T., Hong, W. L., Chitkara, C., Lee, R. W., Ferré, B., et al. (2019). Atypical biological features of a new cold seep site on the Lofoten-Vesterålen continental margin (northern Norway). *Scientific Reports*, *9*(1), 1762. https://doi.org/10.1038/s41598-018-38070-9
Sheppard, S., & Gilg, H. (1996). Stable isotope geochemistry of clay minerals. *Clay Minerals*, *31*(1), 1–24. https://doi.org/10.1180/claymin.1996.031.1.01
Siegel, J., Person, M., Dugan, B., Cohen, D., Lizarralde, D., & Gable, C. (2014). Influence of late Pleistocene glaciations on the hydrogeology of the continental shelf offshore Massachusetts, USA. *Geochemistry, Geophysics, Geosystems*, *15*, 4651–4670. https://doi.org/10.1002/2014GC005569
Solomon, E. A., & Kastner, M. (2012). Progressive barite dissolution in the Costa Rica forearc—Implications for global fluxes of Ba to the volcanic arc and mantle. *Geochimica Et Cosmochimica Acta*, *83*, 110–124. https://doi.org/10.1016/j.gca.2011.12.021
Storrø, G. (2012). "Hydrogeologiske og maringeologiske undersøkelser av Nordbreigrunnen i Meløy kommune, Nordland fylke." NGU-rapport Available online: https://www.ngu.no/publikasjon/hydrogeologiske-og-maringeologiske-unders-kelser-av-nordbreigrunnen-i-mel-y-kommune(2012.035): 13.
Svendsen, J. I., Alexanderson, H., Astakhov, V. I., Demidov, I., Dowdeswell, J. A., Funder, S., et al. (2004). Late Quaternary ice sheet history of northern Eurasia. *Quaternary Science Reviews*, *23*(11-13), 1229–1271. https://doi.org/10.1016/j.quascirev.2003.12.008
Taniguchi, M., Burnett, W. C., Cable, J. E., & Turner, J. V. (2002). Investigation of submarine groundwater discharge. *Hydrological Processes*, *16*(11), 2115–2129. https://doi.org/10.1002/hyp.1145
Tasrianto, R., & Escalona, A. (2015). Rift architecture of the Lofoten-Vesterålen margin, offshore Norway. *Marine and Petroleum Geology*, *64*, 1–16. https://doi.org/10.1016/j.marpetgeo.2015.02.036
Tomaru, H., Torres, M. E., Matsumoto, R., & Borowski, W. S. (2006). Effect of massive gas hydrate formation on the water isotopic fractionation of the gas hydrate system at Hydrate Ridge, Cascadia margin, offshore Oregon. *Geochemistry Geophysics Geosystems*, *7*, Q10001. https://doi.org/10.1029/2005GC001207
Torres, M. E., Brumsack, H. J., Bohrmann, G., & Emeis, K. C. (1996). Barite fronts in continental margin sediments: A new look at barium remobilization in the zone of sulfate reduction and formation of heavy barites in diagenetic fronts. *Chemical Geology*, *127*(1-3), 125–139. https://doi.org/10.1016/0009-2541(95)00090-9
Torres, M. E., McManus, J., & Huh, C. A. (2002). Fluid seepage along the San Clemente Fault scarp: basin-wide impact on barium cycling. *Earth and Planetary Science Letters*, *203*(1), 181–194. https://doi.org/10.1016/S0012-821X(02)00800-2
Tsikalas, F., Inge Faleide, J., & Eldholm, O. (2001). Lateral variations in tectono-magmatic style along the Lofoten–Vesterålen volcanic margin off Norway. *Marine and Petroleum Geology*, *18*(7), 807–832. https://doi.org/10.1016/S0264-8172(01)00030-7
Uemura, T., Taniguchi, M., & Shibuya, K. (2011). Submarine groundwater discharge in Lützow-Holm Bay, Antarctica. *Geophysical Research Letters*, *38*, L08402. https://doi.org/10.1029/2010GL046394
Valentine, D. L., Chidthaisong, A., Rice, A., Reeburgh, W. S., & Tyler, S. C. (2004). Carbon and hydrogen isotope fractionation by moderately thermophilic methanogens. *Geochimica Et Cosmochimica Acta*, *68*(7), 1571–1590. https://doi.org/10.1016/j.gca.2003.10.012
Voelker, A. H. L., Colman, A., Olack, G., Waniek, J. J., & Hodell, D. (2015). Oxygen and hydrogen isotope signatures of Northeast Atlantic water masses. *Deep Sea Research Part II: Topical Studies in Oceanography*, *116*, 89–106. https://doi.org/10.1016/j.dsr2.2014.11.006
Von Damm, K., Edmond, J., Grant, B., Walden, B., & Weiss, R. (1985). Chemistry of submarine hydrothermal solutions at 21°N, East Pacific Rise. *Geochimica Et Cosmochimica Acta*, *49*(11), 2197–2220. https://doi.org/10.1016/0016-7037(85)90222-4
Waelbroeck, C., Labeyrie, L., Michel, E., Duplessy, J. C., McManus, J. F., Lambeck, K., et al. (2002). Sea-level and deep water temperature changes derived from benthic foraminifera isotopic records. *Quaternary Science Reviews*, *21*(1-3), 295–305. https://doi.org/10.1016/S0277-3791(01)00101-9
Wallmann, K., Riedel, M., Hong, W. L., Patton, H., Hubbard, A., Pape, T., et al. (2018). Gas hydrate dissociation off Svalbard induced by isostatic rebound rather than global warming. *Nature communications*, *9*(1), 83. https://doi.org/10.1038/s41467-017-02550-9
You, C.-F., Castillo, P., Gieskes, J., Chan, L., & Spivack, A. (1996). Trace element behavior in hydrothermal experiments: Implications for fluid processes at shallow depths in subduction zones. *Earth And Planetary Science Letters*, *140*(1-4), 41–52. https://doi.org/10.1016/0012-821X(96)00049-0
Zektser, I. S., & Loaiciga, H. A. (1993). Groundwater fluxes in the global hydrologic cycle: past, present and future. *Journal of Hydrology*, *144*(1-4), 405–427. https://doi.org/10.1016/0022-1694(93)90182-9
Zhou, Y., Sawyer, A. H., David, C. H., & Famiglietti, J. S. (2019). Fresh submarine groundwater discharge to the near-global coast. *Geophysical Research Letters*. https://doi.org/10.1029/2019GL082749

References From the Supporting Information

Baeten, N. J., Laberg, J. S., Vanneste, M., Forsberg, C. F., Kvalstad, T. J., Forwick, M., et al. (2014). Origin of shallow submarine mass movements and their glide planes—Sedimentological and geotechnical analyses from the continental slope off northern Norway. *Journal of Geophysical Research: Earth Surface*, *119*, 2335–2360. https://doi.org/10.1002/2013JF003068
Boudreau, B. P. (1997). *Diagenetic models and their implementation: modeling transport and reactions in aquatic sediments*. Berlin: Springer. https://doi.org/10.1007/978-3-642-60421-8

Cheng, H., Edwards, R. L., Shen, C.-C., Polyak, V. J., Asmerom, Y., Woodhead, J., et al. (2013). Improvements in ^{230}Th dating, ^{230}Th and ^{234}U half-life values, and U–Th isotopic measurements by multi-collector inductively coupled plasma mass spectrometry. *Earth and Planetary Science Letters*, *371*, 82–91.

Cremiere, A., Lepland, A., Chang, S., Sahy, D., Condon, D. J., Noble, S. R., et al. (2016). Timescales of methane seepage on the Norwegian margin following collapse of the Scandinavian ice sheet. *Nature communications.*, *7*(1). https://doi.org/10.1038/ncomms11509

Edwards, R. L., Chen, J., & Wasserburg, G. (1987). ^{238}U-^{234}U-^{230}Th-^{232}Th systematics and the precise measurement of time over the past 500,000 years. *Earth And Planetary Science Letters*, *81*(2-3), 175–192. https://doi.org/10.1016/0012-821X(87)90154-3

EPA, C. (1983). "EPA 600/4-79-020 Methods for Chemical Analysis of Water and Wastes". Retrieved from http://www.wbdg.org/ffc/epa/criteria/epa-600-4-79-020

Forwick, M., S.-I. Nam, K. Husum and S. Iversen (2017). "2016 RV Helmer Hanssen cruise report: Marine-geological cruise to west Spitsbergen fjords."

Hong, W.-L., Torres, M. E., Carroll, J., Crémière, A., Panieri, G., Yao, H., & Serov, P. (2017). shallow marine gas hydrate reservoir is insensitive to momentary ocean warming. *Nature communications*, *8*(1), 15745. https://doi.org/10.1038/ncomms15745

International Atomic Energy Agency (2018). "Global Network of Isotopes in Precipitation." The GNIP Database: https://nucleus.iaea.org/wiser.

Kharaka, Y. K., & Mariner, R. H. (1989). *Chemical geothermometers and their application to formation waters from sedimentary basins. Thermal history of sedimentary basins*, (pp. 99–117). Springer. https://doi.org/10.1007/978-1-4612-3492-0_6

Kiss, E. (1988). Ion-exchange separation and spectrophotometric determination of boron in geological materials. *Analytica Chimica Acta*, *211*, 243–256. https://doi.org/10.1016/S0003-2670(00)83684-3

Pohjola, V. A., Martma, T. A., Meijer, H. A., Moore, J. C., Isaksson, E., Vaikmäe, R., & Van De Wal, R. S. (2002). Reconstruction of three centuries of annual accumulation rates based on the record of stable isotopes of water from Lomonosovfonna, Svalbard. *Annals of Glaciology*, *35*, 57–62. https://doi.org/10.3189/172756402781816753

Rae, J. W., Foster, G. L., Schmidt, D. N., & Elliott, T. (2011). Boron isotopes and B/Ca in benthic foraminifera: proxies for the deep ocean carbonate system. *Earth and Planetary Science Letters*, *302*(3-4), 403–413. https://doi.org/10.1016/j.epsl.2010.12.034

Rise, L., Bøe, R., Riis, F., Bellec, V. K., Laberg, J. S., Eidvin, T., et al. (2013). The Lofoten-Vesterålen continental margin, North Norway: Canyons and mass-movement activity. *Marine and Petroleum Geology*, *45*, 134–149. https://doi.org/10.1016/j.marpetgeo.2013.04.021

Seeberg-Elverfeldt, J., Schlüter, M., Feseker, T., & Kölling, M. (2005). Rhizon sampling of porewaters near the sediment-water interface of aquatic systems. *Limnology and Oceanography: Methods*, *3*(8), 361–371.

Tishchenko, P., Hensen, C., Wallmann, K., & Wong, C. S. (2005). Calculation of the stability and solubility of methane hydrate in seawater. *Chemical Geology*, *219*(1-4), 37–52. https://doi.org/10.1016/j.chemgeo.2005.02.008

Wallace, P. J., G. R. Dickens, C. K. Paull and W. Ussler (2000). Effects of core retrieval and degassing on the carbon isotope composition of methane in gas hydrate- and free gas-bearing sediments from Blake Ridge. Proceedings of the Ocean Drilling Program, Scientific Results. C. K. Paul, R. Matumoto, P. J. Wallace and W. P. Oillon. 164.

Whiticar, M. J. (1999). Carbon and hydrogen isotope systematics of bacterial formation and oxidation of methane. *Chemical Geology*, *161*(1-3), 291–314. https://doi.org/10.1016/S0009-2541(99)00092-3